Coupled Systems Mechanics, *Vol. 14, No. 6 (2025) 507-530*
https://doi.org/10.12989/csm.2025.14.6.507

Dynamic response prediction of vehicle-bridge system under random excitation based on SSA-LSTM model

Tian Zhang*[1], Yuanzhu Liu[1], Pengfei Li[2] and Yunfeng Zou[3,4]

[1]*Transportation Engineering College, Dalian Maritime University, Dalian 116026, China*
[2]*Research Institute of Highway Ministry of Transport, Beijing 100088, China*
[3]*National Engineering Research Center of High-speed Railway Construction Technology, Changsha 410075, China*
[4]*School of Civil Engineering, Central South University, Changsha 410075, China*

(Received July 30, 2025, Revised October 28, 2025, Accepted November 11, 2025)

Abstract. To establish digital twin model of the vehicle-bridge interaction system under random track irregularity excitation, it is necessary to compute the system response in real time. Traditional methods are time-intensive and lack real-time capability, whereas surrogate model-based approaches can rapidly and accurately predict dynamic response. This study proposes a surrogate model that employs the Sparrow Search Algorithm to optimize Long Short-Term Memory neural networks for predicting the dynamic response of vehicle-bridge interaction system under random excitation. Initially, a physical model of the vehicle-bridge interaction system is established, incorporating track irregularities to calculate the dynamic response and generate training samples. Subsequently, an SSA-LSTM surrogate model is developed and trained. Finally, the surrogate model is utilized to predict the dynamic response of the vehicle-bridge interaction system under arbitrary track irregularity excitations. To validate the robustness of the proposed algorithm, the prediction results of various surrogate models are compared. The results indicate that the proposed surrogate model achieves higher computational efficiency compared to classical mechanical models of the vehicle-bridge interaction system. Moreover, the SSA-LSTM surrogate model outperforms traditional LSTM and Backpropagation surrogate models in terms of prediction accuracy for the dynamic response of the vehicle-bridge interaction system.

Keywords: dynamic response prediction; random excitation; sparrow search algorithm; surrogate model; vehicle-bridge interaction system

1. Introduction

With the continuous increase in train operating speed and the increasing lightweight design of vehicles, track irregularity, as one of the primary excitation sources between vehicle and bridge subsystems, can significantly influence the safety and comfort of train operations on bridges (Xia and Zhang 2003, Rocha and Henriques 2015, Wang 2019). Early studies mostly focused on simplified models, such as simplifying the vehicle-bridge interaction system into a moving load

*Corresponding author, Professor, E-mail: saghb@126.com

 ISSN: 2234-2184 (Print), 2234-2192 (Online)

model or moving mass model (Xiao and Shen 2005, Xiao and Zhu 2007). Later studies were carried out on moving spring mass model, quarter vehicle suspensions system and whole vehicle systems (Li and Xu 2010, Deng and Duan 2015, Gui and Zhu 2019). Theoretical and numerical analyses are carried out using the above model, and field tests are executed. Subsequently, the research gradually extended to long-span bridges like the Continuous Girder Bridges, the Cable-stayed bridges, the Suspension Bridges and other complex bridge structures (Dong 2019, Zhou and Xue 2023, Ning and Deng 2024). The theoretical model has developed from a single elastic model to a complex model including nonlinear, viscoelastic and dynamic contact factors. Research methods have also developed from the initial analytical method to modern numerical simulation techniques, such as the Finite Element Method (FEM) and Dynamics of Multi-Body System (MBD) (Chen 2022, Wang and Zhang 2024). Meanwhile, significant progress has also been made in bridge inspection methods utilizing vehicle-based scanning techniques founded on vehicle-bridge interaction vibration theory. This approach treats passing vehicles as mobile sensors, indirectly identifying dynamic characteristics of bridges and assessing structural health conditions by measuring the dynamic responses of the vehicles. Since the concept was systematically proposed by Yang *et al.* (Yang and Lin 2004) in 2004, related research has continuously deepened. As systematically summarized in the review by Yang *et al.* (Yang and Yang 2017). The focus of studies has expanded from initial frequency identification (Malekjafarian and McGetrick 2015) to damping identification, damage detection, and condition assessment based on intelligent algorithms (Ni and Mao 2023, Shi and Yang 2025). In recent years, as described by Wang *et al.* (Wang and Yang 2022) research has further integrated intelligent algorithms such as deep learning, propelling the state assessment into a new stage. However, practical application of this method still faces challenges, such as the low signal-to-noise ratio of bridge modal information in vehicle responses, interference from environmental noise, and uncertainties introduced primarily by road/rail surface irregularities as a major excitation source. Due to the stochastic nature of the time at which the train crosses the bridge and the varying degrees of track wear caused by repeated train passage, the track irregularity excitation acting on the vehicle-bridge interaction system can be considered a random process, thereby inducing stochastic characteristics in the system dynamic response. Therefore, it is essential to investigate the dynamic behavior of the vehicle-bridge interaction system under random track irregularity excitation (Li and Xiang 2018, Li and Wang 2015). Currently, some scholars have investigated the dynamic response of trains under random excitation using random vibration approaches such as the virtual excitation method, response surface method, and probability density evolution method, achieving certain results (Zhu 2014, Li and Zhu 2012, Liu and Zhang 2018). However, existing numerical simulation techniques are not well suited for large-scale bridge structures due to their high number of degrees of freedom, which results in prolonged computation times and hinders real-time result feedback. This limitation is particularly critical in the current application of digital twin technology within the field of vehicle–bridge interaction vibration analysis. Therefore, there is an urgent need to develop an efficient and accurate method for calculating the dynamic response of vehicle–bridge interaction system under random excitation.

In recent years, artificial intelligence algorithms have undergone rapid development (Wang and Tan 2003, Simpson and Peplinski 2001). Breakthroughs in the research of Artificial Neural Networks (ANN) have provided new approaches for addressing complex nonlinear and uncertain system response problems. For example, basic neural network models such as Backpropagation neural networks and Radial Basis Function neural networks have been employed to predict dynamic responses in linear or weakly nonlinear systems (Du and Guo 2006). The rapid

advancement of deep neural networks has revitalized artificial intelligence research, with algorithms such as machine learning and deep learning now widely applied in nonlinear structural dynamics simulations (Tang and Dong 2006). In the field of bridge seismic engineering, Liao and Zhang (2021) proposed a data-driven modeling approach based on Stacked Residual Long Short-Term Memory neural networks (Res-LSTM) to predict nonlinear seismic responses of bridges, with the predicted results satisfying the required accuracy. Kim and Kwon (2019) introduced a Convolutional neural network model for predicting structural responses under seismic excitation, which has the potential to eliminate the need for nonlinear time history analysis in the future. Hu and Guo (2024) reconstructed unmeasurable or missing structural response data during earthquakes using a Physics-informed neural network that incorporates prior knowledge, which has significant implications for structural health monitoring and safety assessment. In the field of bridge wind engineering, Wang and Wu (2020) proposed a knowledge-enhanced deep learning algorithm to predict nonlinear structural dynamic responses induced by wind fields. Fang and Tang (2020) applied neural networks to analyze and predict bridge responses under combined wind and wave loads. Xu and Chen (2021) established a mapping model between wind field parameters and structural buffeting responses using neural networks, enabling the prediction of bridge buffeting behavior. In the domain of vehicle-bridge interaction vibrations, Li and Wang (2021, 2023) introduced a deep learning framework for predicting the dynamic responses of bridge system under vehicle loads, thereby initiating research on neural network models in this field. Li *et al.* (Li and Wang 2022) investigated the performance of convolutional neural networks (CNN), long short-term memory networks (LSTM), and bidirectional LSTM models in predicting the time history of vehicle-induced bridge responses, providing important theoretical basis and comparison benchmarks for selecting the most suitable deep learning architecture in different engineering scenarios. Mao and Li (2023) optimized the Long Short-Term Memory (LSTM) neural network using the particle swarm optimization algorithm to predict the stochastic vibration responses of heavy-haul railway vehicle–track–bridge system, providing foundational insights and references for the study of stochastic vibration responses in vehicle–bridge interaction system. Han (2022) investigated the impact of random vehicle parameters on vehicle–bridge responses through the PC-ARMIX surrogate model. He and Zhao (2024) considered the randomness of track structure parameters in the vehicle–track–bridge interaction system and proposed a surrogate model based on a Backpropagation (BP) neural network optimized by the Sparrow Search Algorithm, which demonstrated higher computational efficiency. Subsequently, a BiLSTM-AM model was proposed to inversely identify track irregularities from vehicle responses, offering a novel approach for reconstructing excitation sources based on vehicle dynamic responses. This model focuses on the inverse identification of excitations through vehicle responses, demonstrating complementarity with the methodology presented in this study (He and Zhao 2025).

Currently, research on dynamic response prediction of vehicle–bridge interaction system based on deep learning remains limited, particularly under stochastic excitation. Therefore, further development is needed to apply deep learning algorithms for predicting dynamic responses of vehicle–bridge interaction system under stochastic excitation. This paper proposes a surrogate model based on an LSTM neural network optimized by the Sparrow Search Algorithm to predict the dynamic response of the vehicle–bridge interaction system under random track irregularities. The method constructs the surrogate model with random track irregularities as input and the dynamic responses of the bridge or vehicle as output. The Sparrow Search Algorithm optimizes the structural parameters of the LSTM model, thereby enhancing prediction accuracy. The prediction results are evaluated using correlation coefficients, root mean square errors, and other

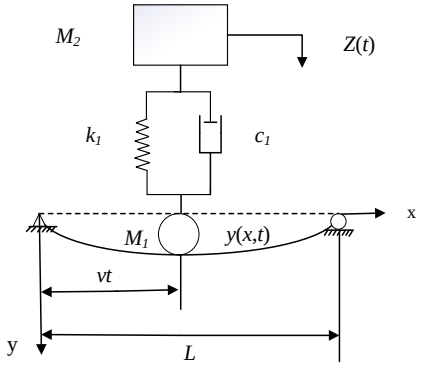

Fig. 1 Vehicle-bridge interaction system physical model

performance metrics, and are validated by comparison with analytical model calculations. Finally, the findings are discussed and summarized.

2. Physical model of vehicle-bridge interaction system

Due to the complexity of vibration analysis in actual vehicle-bridge interaction systems, this paper simplifies the system into a representative moving spring-mass model to verify the effectiveness of the proposed surrogate model in predicting the dynamic response of the system, as illustrated in Fig. 1. The simply supported beam is assumed to have a uniform cross-section with uniformly distributed mass (constant mass m) and viscous damping. The moving vehicle consists of wheels, a vehicle body, springs, and dampers. The mass of the wheel is M_1, and it moves uniformly along the beam without separation, meaning its displacement equals the dynamic displacement $y(x,t)$ of the beam. The mass of the vehicle body is M_2, and its dynamic displacement is denoted as $Z(t)$. The spring stiffness and damping coefficient are represented by k_1 and c_1, respectively.

2.1 Motion differential equation for the Vehicle-bridge interaction system

The vehicle-bridge interaction system model is illustrated in Fig. 1. Let the load of the moving vehicle acting on the simple supported beam be $F(t)$, then the motion equation of the simple supported beam under the action of $F(t)$ is

$$EI\ \frac{\partial^4 y(x,t)}{\partial x^4} + m\frac{\partial^2 y(x,t)}{\partial t^2} + c\frac{\partial y(x,t)}{\partial t} = F(x,t)\delta(x-vt) \tag{1}$$

Where EI is the flexure stiffness of the bridge, c is the damping factor of the bridge, and m is the mass per unit length of the bridge. δ is the Dirac function, when $x=vt$, $\delta=1$, when $x\neq vt$, $\delta=0$.

According to the mode decomposition method, the dynamic displacement $y(x,t)$ of bridge forced vibration be expressed as

$$y(x,t) = \sum_{i=1}^{\infty} \Phi_i(x)\ q_i(t) \tag{2}$$

The *n*-th mode of the simply supported beam be expressed as

$$\Phi_n(x) = \sin\frac{n\pi x}{L} \tag{3}$$

Substitute Eqs. (2) and (3) into Eq. (1), we can obtain

$$\begin{aligned} &EI\sum_{i=1}^{\infty}\frac{d^4\Phi_i(x)}{\partial x^4}q_i(t) + m\sum_{i=1}^{\infty}\Phi_i(x)q_i''(t) + \\ &c\sum_{i=1}^{\infty}\Phi_i(x)q_i'(t) = F(x,t)\delta(x-vt) \end{aligned} \tag{4}$$

The above equation is multiplied by $\Phi_n(x)$ and integrated along the beam length, and the vibration equation of the *n*-th mode can be obtained due to the orthogonality of the mode

$$q_n''(t) + 2\xi_n\omega_n q_n'(t) + \omega_n{}^2 q_n(t) = \frac{2}{mL}\int_0^L F(x,t)\delta(x-vt)\Phi_n(x)dx \tag{5}$$

In the formula, $\omega_n = \left(\frac{n\pi}{L}\right)^2\sqrt{\frac{EI}{m}}$ is the n order natural vibration circular frequency of the simply supported beam; $\xi_n = \frac{c}{2m\omega_n}$ is the modal damping ratio of the *n*-th mode.

At this juncture, random track irregularities are introduced, assuming the vertical displacement of car body M_2 as $Z(t)$, where the simply supported beam is subjected to the following force

$$\begin{aligned} F(x,t) &= M_1 g + M_2 g - M_1\frac{d^2[y(x,t)+\omega(x)]}{dt^2} \\ &+k_1[Z(t)-y(x,t)-\omega(x)] + c_1[Z'(t) - \frac{d[y(x,t)+\omega(x)}{dt}] \end{aligned} \tag{6}$$

In the formula, $\omega(x)$ represents the track irregularity, $\omega(x) = h\cos\left(\frac{4\pi x}{L}\right)$

Among

$$y(x,t)|_{x=vt} = y(vt,t) \tag{7}$$

Therefore

$$\frac{d^2y(x,t)}{dt^2} = \frac{\partial y^2(x,t)}{\partial t^2} + v\frac{\partial y(x,t)}{\partial x} \tag{8}$$

$$\frac{d^2y(x,t)}{dt^2} = \frac{\partial y^2(x,t)}{\partial t^2} + 2v\frac{\partial y^2(x,t)}{\partial x\partial t} + v^2\frac{\partial^2 y(x,t)}{\partial x^2} \tag{9}$$

Substituting Eqs. (6), (7), (8) and (9) into (5) can be obtained

$$q_n''(t) + \alpha_1\sin n\Delta t\sum_{i=1}^{\infty}\sin i\Delta t q_i''(t) + 2\xi_n\omega_n q_n'(t) +$$

$$
\begin{aligned}
&2\alpha_1\Delta \sin n\Delta t\sum_{i=1}^{\infty} i\cos i\Delta tq_i'(t)+\alpha_c \sin n\Delta t\sum_{i=1}^{\infty} \sin i\Delta tq_i'(t)+\\
&\omega_n{}^2q_n'(t)-\alpha_1\Delta^2 \sin n\Delta t\sum_{i=1}^{\infty} i^2 \sin i\Delta tq_i(t)+\alpha_k \sin n\Delta t\sum_{i=1}^{\infty} \sin i\Delta tq_i(t)\\
&+\alpha_c\Delta \sin n\Delta t\sum_{i=1}^{\infty} i\cos i\Delta tq_i(t)-\alpha_k \sin n\Delta tZ(t)-\alpha_c \sin n\Delta tZ'(t)\\
&=(\alpha_1+\alpha_2)g\sin n\Delta t+\frac{2h}{mL}[m_1(4\Delta)^2\cos(4\Delta t)-k_1\cos(4\Delta t)\\
&+4c_1\Delta\sin(4\Delta t)]\sin(n\Delta t)
\end{aligned}
\tag{10}
$$

in which,

$$
\alpha_1=\frac{2M_1}{mL},\ \alpha_2=\frac{2M_2}{mL},\ \alpha_k=\frac{2k_1}{mL},\ \alpha_c=\frac{2c_1}{mL},\ \Delta=\frac{\pi v}{L},
$$

g is the gravitational acceleration.

The dynamic balance equation of vehicle body mass M_2 is given

$$
M_2Z''(t)+k_1\left[Z(t)-y(x,t)-\omega(x)\right]+c_1\left[Z'(t)-\frac{dy(x,t)}{dt}-\omega(x)\right]=0 \tag{11}
$$

Substituting Eqs. (7) and (8) into (11), we can obtain

$$
\begin{aligned}
&M_2Z''(t)+c_1Z'(t)+k_1Z(t)-k_1\sum_{i=1}^{\infty} \sin i\Delta tq_i(t)-c_1\sum_{i=1}^{\infty} \sin i\Delta tq_i'(t)\\
&-c_1\Delta\sum_{i=1}^{\infty} i\cos i\Delta tq_i(t)=0
\end{aligned}
\tag{12}
$$

Let the number of modes in Eq. (13) be N, and Eqs. (10) and (12) can be writen in matrix form

$$
[M]\{\eta''(t)\}+[C]\{\eta'(t)\}+[K]\{\eta(t)\}=\{P(t)\} \tag{13}
$$

in which,

$$
\{\eta(t)\}=\left[q_1(t)\ q_2(t)\ \cdots\ q_n(t)\ \cdots\ q_N(t)\ Z(t)\right]^T
$$

$$
\{P\}=\left[f_1\ f_2\ \cdots\ f_i\ \cdots\ f_N(t)\ 0\right]^T,
$$

$$
f_i=(\alpha_1+\alpha_2)gD_i+h[\alpha_1(4\Delta)^2\cos(4\Delta t)-\alpha_k\cos(4\Delta t)+4\alpha_c\Delta\sin(4\Delta t)]
$$

$$
[M]=\begin{bmatrix}
m_{11} & m_{1i} & \cdots & m_{1N} & 0\\
m_{21} & m_{ii} & \cdots & m_{2N} & 0\\
\cdots & \cdots & \ddots & \cdots & \cdots\\
m_{N1} & m_{Ni} & \cdots & m_{NN} & 0\\
0 & 0 & \cdots & 0 & M_2
\end{bmatrix}
$$

$$
m_{ij}=\alpha_1D_{ij}(i\neq j),\ m_{ii}=1+\alpha_1D_{ii};
$$

$$[C]=\begin{bmatrix} c_{11} & c_{1i} & \cdots & c_{1N} & -\alpha_c D_1 \\ c_{1i} & c_{ii} & \cdots & c_{2N} & -\alpha_c D_i \\ \cdots & \cdots & \ddots & \cdots & \cdots \\ c_{N1} & c_{Ni} & \cdots & c_{NN} & -\alpha_c D_N \\ -c_1 D_1 & -c_1 D_1 & \cdots & -c_1 D_1 & c_1 \end{bmatrix}$$

$$c_{ij}=2\alpha_1\Delta E_{ij}+\alpha_c D_{ij}(i\neq j),\ c_{ii}=2\xi_i\omega_i+2\alpha_1\Delta E_{ii}+\alpha_c D_{ii};$$

$$[K]=\begin{bmatrix} k_{11} & k_{1i} & \cdots & k_{1N} & -\alpha_k D_1 \\ k_{i1} & k_{ii} & \cdots & k_{2N} & -\alpha_k D_i \\ \cdots & \cdots & \ddots & \cdots & \cdots \\ k_{N1} & k_{Ni} & \cdots & k_{NN} & -\alpha_k D_N \\ -k_1 D_1 - c_1\Delta E_1 & -k_1 D_i - c_1\Delta E_i & \cdots & -k_1 D_N - c_1\Delta E_N & k_1 \end{bmatrix}$$

$$k_{ij}=-\alpha_1\Delta^2 G_{ij}+\alpha_k D_{ij}+\alpha_c\Delta E_{ij}(i\neq j),\ k_{ii}=\omega^2{}_i-\alpha_1\Delta^2 G_{ii}+\alpha_k D_{ii}+\alpha_c\Delta E_{ii};$$

$$D_i=\sin i\Delta t,\ D_{ij}=D_iD_j=\sin i\Delta t\sin j\Delta t,\ E_i=i\cos i\Delta t,\ G_i=i^2\sin i\Delta t,$$

$$E_{ij}=D_iE_j=\sin i\Delta t\times j\cos j\Delta t,\ G_{ij}=D_iG_j=\sin i\Delta t\times j^2\sin j\Delta t.$$

2.2 Simulation of random track irregularity

Track irregularity is one of the primary excitation sources in the vehicle-bridge interaction system. It acts as an inherent self-excitation mechanism within the system and has a direct impact on both operational safety and ride comfort during train movement. Due to its strong stochastic nature, track irregularity cannot be explicitly described by deterministic mathematical expressions. In the literature, the spatial power spectral density (PSD) function is commonly used to characterize the statistical properties of track irregularity samples. Widely recognized track irregularity spectra include the American spectrum, the German high-speed track spectrum, and the Chinese high-speed railway track irregularity spectrum. In this study, the Chinese high-speed railway track irregularity spectrum is adopted for subsequent vibration analysis of the vehicle-bridge interaction system (Yu and Mao 2015). The track spectrum specified in the "High-Speed Railway Track Irregularity Spectrum" is formulated as a power spectral density function with units of mm²/(1/m), spanning a spatial frequency range of 0.005–0.5 (1/m), which corresponds to wavelengths ranging from 2 to 200 meters. The mathematical expression is as follows

$$S(f)=\frac{A}{f^k} \tag{14}$$

In the formula, f is the spatial frequency (1/m); A and k are fitting coefficients. Subsequently, a representative spatial profile of vertical track irregularity was simulated using the harmonic superposition method in MATLAB, based on the power spectral density specified for Chinese high-speed railway ballastless tracks (Li 2023), as shown in Fig. 2.

2.3 Dynamic response analysis of bridges and vehicles

The simply supported beam in this paper has a span of 32 m, a flexural rigidity of 2.05×10^7 kN·m², and a linear mass of 9.365×10^3 kg/m. The mass of the vehicle body is 4.69×10^4 kg, and the

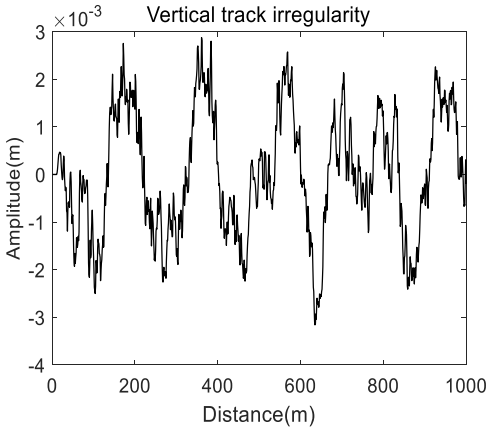

(a) Samples of vertical track irregularity

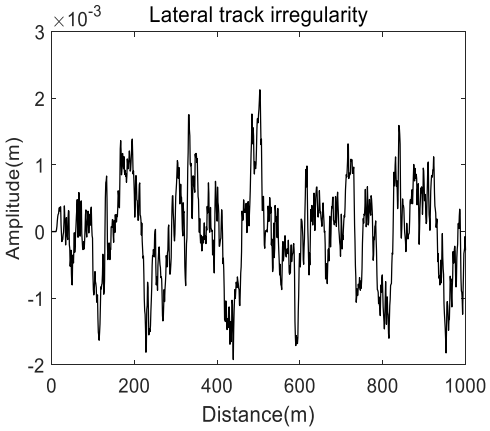

(b) Samples of lateral track irregularity

Fig. 2 Track irregularity samples from Chinese high-speed railways

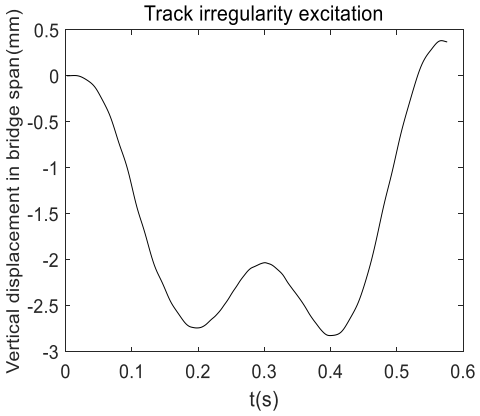

(a) Vertical displacement time curve at mid-span of bridge

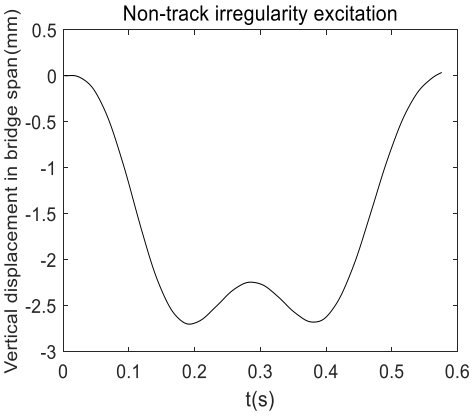

(b) Vertical displacement time curve at mid-span of bridge

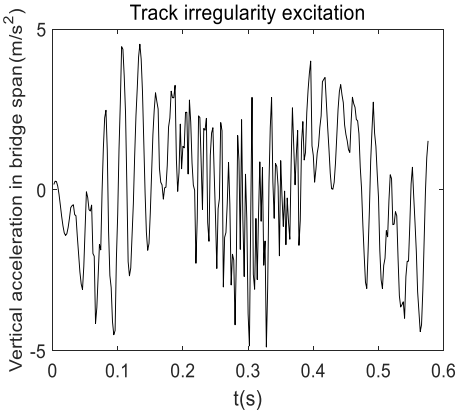

(c) Vertical acceleration time curve at mid-pan of bridge

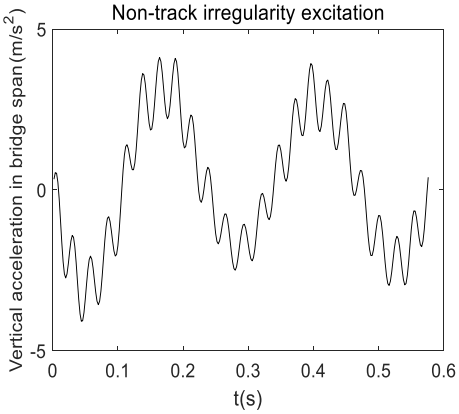

(d) Vertical acceleration time curve at mid-pan of bridge

Fig. 3 Time-history curve of bridge dynamic response

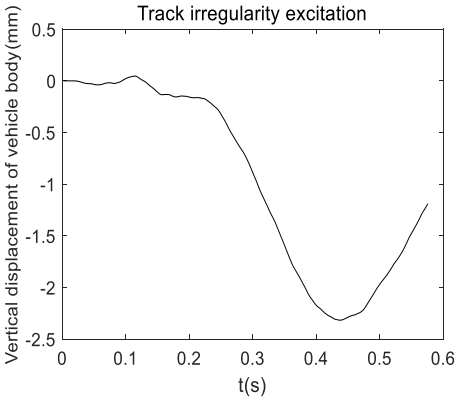

(a) Vertical displacement time curve of vehicle body

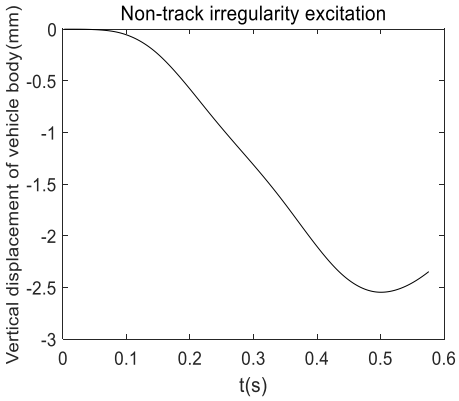

(b) Vertical acceleration time curve of vehicle body

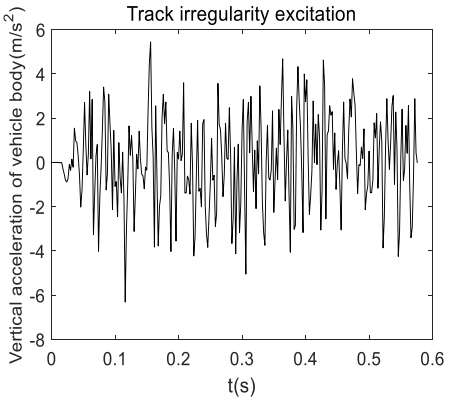

(c) Vertical displacement time curve of vehicle body

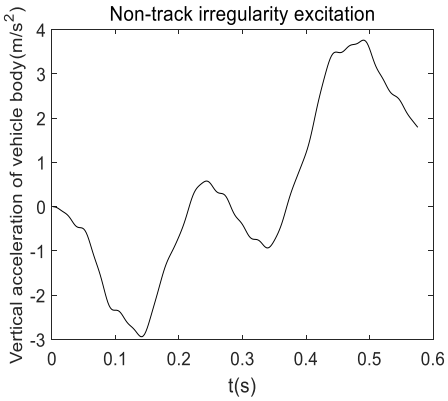

(d) Vertical acceleration time curve of vehicle body

Fig. 4 Time-history curve of vehicle dynamic response

mass of each wheel is 1.69×10^4 kg. The stiffness of the vehicle spring is 4.87×10^6 N/m, and the damping coefficient is 3.14×10^5 N·s/m. These bridge and vehicle parameters are substituted into the equations of motion, which are then solved using the Newmark-β method. Based on the operational speed range of Chinese EMU trains, the dynamic responses of both the bridge and the vehicle are calculated at a speed of 200 km/h, under conditions with and without track irregularity excitation. The response curves include the mid-span vertical displacement and acceleration of the bridge, as well as the vertical displacement and acceleration of the vehicle body, as shown in Figs. 3 and 4.

3. Prediction surrogate model for dynamic response of vehicle-bridge interaction system

3.1 LSTM neural network

Long Short-Term Memory (LSTM) neural network is a specific type of the Recurrent Neural Network (RNN) specifically designed to process and predict time series data. Through its unique

gating mechanism, LSTM effectively solves the problem of gradient disappearance and gradient explosion in long sequences of traditional RNN, which makes it especially good in tasks that need to rely on information for a long time. The LSTM unit is mainly composed of input gate, forget gate, output gate and memory unit, through which the flow of information is controlled. What data is removed from the cell state is decided by the forget gate. The formula is as follows

$$f_t = \sigma\left(W_f \cdot \left[h_{t-1}, x_t\right] + b_f\right) \tag{15}$$

What additional data must be added to the cell state is determined by the input gate. There are two steps:

(1) Generate the candidate values

$$\overline{C_t} = \tanh\left(W_c \cdot \left[h_{t-1}, x_t\right] + b_c\right) \tag{16}$$

(2) Determine the information to be updated

$$i_t = \sigma\left(W_i \cdot \left[h_{t-1}, x_t\right] + b_i\right) \tag{17}$$

Then update the cell status through the forget gate and the input gate

$$C_t = f_t \cdot C_t + i_t \cdot \overline{C}_t \tag{18}$$

The output gate determines what the hidden state (i.e., output) is at the current moment. The formula is as follows

$$o_t = \sigma\left(W_o \cdot \left[h_{t-1}, x_t\right] + b_o\right) \tag{19}$$

Finally, the hidden state of the current moment is obtained by the following formula

$$h_t = o_t \cdot \tanh\left(C_t\right) \tag{20}$$

Where f_t, i_t, o_t represents the forgetting door, input door and output door; σ represents the sigmoid activation function; W_f, W_c, W_i, W_o represents the weight matrix of the door response; $\overline{C}_t$ represents the indicates generating candidate values; C_t represents the state unit; h_{t-1} is the hidden state of the last moment; x_t is the current input; b_f, b_c, b_i, b_o represents the offset item of the door response. The unit structure diagram of LSTM is shown in Fig. 5, where A represents the memory unit of the neural network layer.

3.2 Optimization of LSTM neural network based on Sparrow Search Algorithm (SSA-LSTM)

Sparrow Search Algorithm (SSA) is a novel optimization algorithm based on swarm intelligence, motivated by sparrow anti-predation and foraging habits. By simulating the social relations and behavior patterns of sparrows during foraging, the algorithm provides an effective method to solve complex optimization problems. By optimizing the hidden unit number, maximum training period, initial learning rate and regularization parameters of LSTM neural network, the prediction of the model can be improved and the neural network can be prevented from overfitting. The major step of the SSA algorithm is as follows: Firstly, the population is initialized, and the positions of N_0 individual sparrows are randomly generated to form population

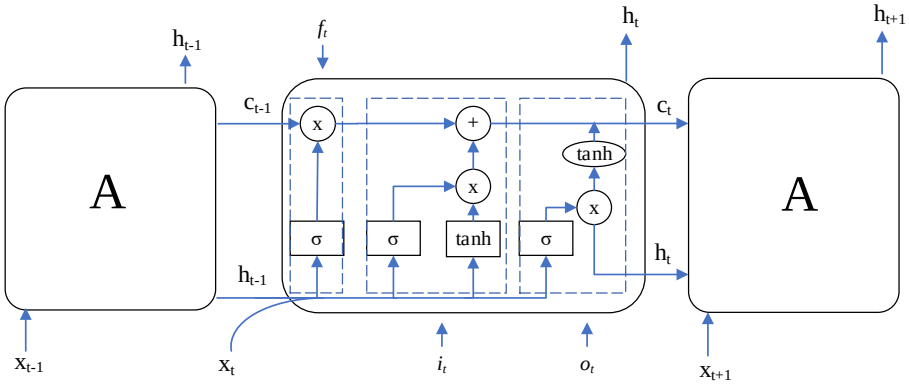

Fig. 5 LSTM neural network structure diagram

$X=\{x_1,x_2;\cdots x_n\}$. Each individual position represents a candidate solution. The positions of each individual represent a candidate solution. Then the fitness evaluation is carried out to calculate the fitness value of each individual's position under the objective function $f(x)$. Then the location of the foragers is updated, and the foragers are selected according to the proportion of the foragers (generally 20% of the population), and the location of the foragers is updated.

$$x_i(t+1)=\begin{cases} x_i(t)\cdot e^{-\frac{i}{\alpha D}} & r_2<st \\ x_i(t)+K_0\cdot\left(x_j(t)-x_k(t)\right) & r_2>st \end{cases} \tag{21}$$

Where: r_2 is a random number, st is a security threshold, K_0 is a random number, j and k are two different individuals, $\alpha(\alpha\in[0,1])$ is a random number; D is the maximum number of iterations.

Then update the location of the foraging follower. The formula for updating the location of the foraging follower is as follows

$$x_i(t+1)=Q_0\cdot x_w(t)+\beta\cdot\left|x_i(t)-x_w(t)\right| \tag{22}$$

Where: Q_0 and β are a random number and x_w is the position of the optimal individual in the current population.

When sparrows feel threatened by predators, they will perform position updates to avoid threats and conduct anti-predation

$$x_i(t+1)=x_{\min}+R\cdot\left(x_{\max}-x_{\min}\right) \tag{23}$$

Where: $x_{\max}$ and $x_{\min}$ is the smallest and largest individual in the current population respectively, and is a random number.

Repeat the above steps until a preset number of iterations is met or convergence conditions are reached.

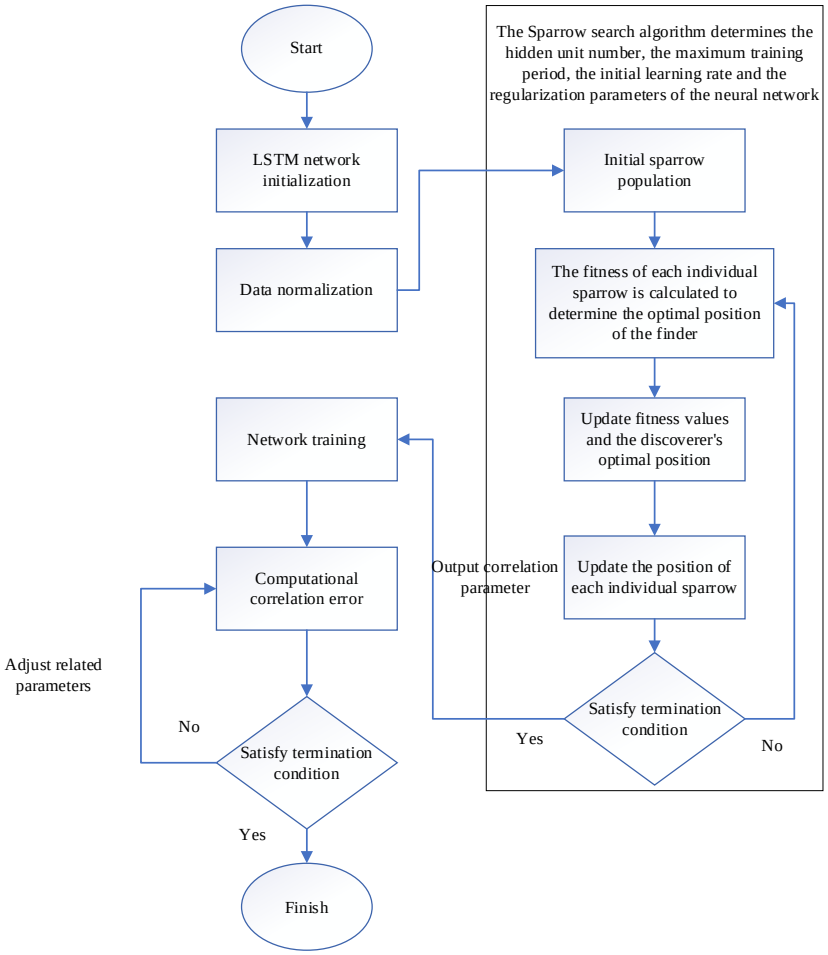

Fig. 6 SSA-LSTM neural network flowchart

The calculation flow chart of SSA-LSTM neural network is shown in Fig. 6. The specific calculation steps are as follows:

(1) Normalization of the original data;

(2) Initialize sparrow population number, initial location, optimal location, optimal fitness and other main parameters;

(3) Formulas (21)-(23) were used to calculate the position of each individual sparrow, update the fitness value and the optimal location of the finder, and determine whether the termination condition is met. If yes, the optimal LSTM neural network hidden unit number, maximum training period, initial learning rate and regularization parameters are output; otherwise, the initial steps are returned.

(4) Training, prediction and evaluation of LSTM neural network.

The SSA is used to optimize the number of hidden units, the maximum training period, the initial learning rate and the regularization parameters in the LSTM neural network model to realize the organic combination of the vehicle-bridge insteraction system model and the neural network model.

3.3 SSA-LSTM prediction process and evaluation indicators

The specific prediction steps of the SSA-LSTM surrogate model for forecasting the dynamic response of the vehicle-bridge interaction system are as follows. First, the motion equation of the vehicle-bridge interaction system is established. Considering that random track irregularity excitation has a significant influence on the dynamic response of both the bridge and the vehicle during train passage, 80 groups of randomly generated track irregularity excitations are selected as input samples for the surrogate model to ensure estimation accuracy. Next, these random excitations are substituted into the motion equation to compute the corresponding dynamic responses of the vehicle or bridge, which serve as the output samples for the surrogate model. The vehicle speed is varied within the operational range of Chinese high-speed railway EMUs, i.e., 200–250 km/h. Subsequently, training data are constructed based on the above computational results, and the SSA-LSTM surrogate model is developed to predict the dynamic response of the vehicle-bridge system. Finally, a new set of track irregularity excitation is provided, and the surrogate model is used to predict the dynamic response at various speeds. The prediction results are then compared with the analytical calculation results to evaluate the computational efficiency and predictive accuracy of the proposed surrogate model.

In the LSTM model, a two-hidden-layer architecture is employed, where the first hidden layer contains H_1 neurons and the second hidden layer contains H_2 neurons. The number of training samples s is set to 400, the number of training iterations e is set to 1000, and the initial learning rate η is set to 0.01. The convergence error is defined as 1×10^{-5}. Input data are normalized to the range [–1, 1], and the learning rate is updated every 100 epochs. The training set and validation set are divided in a 7:3 ratio. In the SSA-LSTM model, the sparrow population size z is set to 5, and the maximum number of iterations x is set to 10. Among the population, 20% are designated as discoverers, and the remaining are joiners. The warning threshold is set to 0.8. When the warning value is below 0.8, no predator threat exists, and the sparrows continue foraging in the current area; otherwise, a predator threat is present, and the sparrows must relocate for foraging. The search ranges for the sparrow search algorithm optimizing the LSTM parameters H_1, H_2, e, and η are [1, 100], [1, 100], [1, 1000], and [0.001, 0.01], respectively.

To evaluate and compare the prediction accuracy of different surrogate models, this paper employs four error evaluation metrics: root mean square error (RMSE), mean absolute error (MAE), mean absolute percentage error (MAPE), and coefficient of determination (R^2). RMSE quantifies the magnitude of the prediction errors, MAE measures the average absolute error, MAPE reflects the average percentage error across observations, and R^2 indicates the proportion of variance in the observed values that can be explained by the model. The mathematical formulations of these metrics are as follows

$$\mathrm{RMSE}=\sqrt{\frac{1}{m}\sum_{i=1}^{m}\left(y_i-\hat{y}_i\right)^2} \tag{24}$$

$$\mathrm{MAE}=\frac{1}{m}\sum_{i=1}^{m}\left|y_i-\hat{y}_i\right| \tag{25}$$

$$\mathrm{MAPE}=\frac{1}{m}\sum_{i=1}^{m}\left|\frac{y_i-\hat{y}_i}{y_i}\right|\times100\% \tag{26}$$

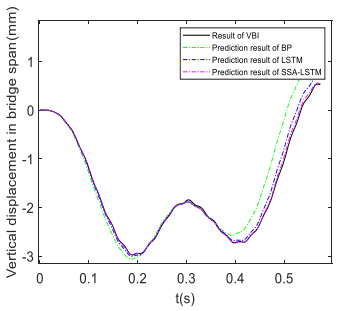

(a) Prediction results

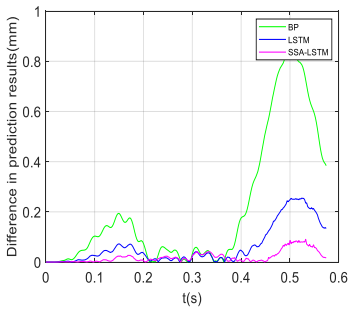

(b) Errors in predicted values

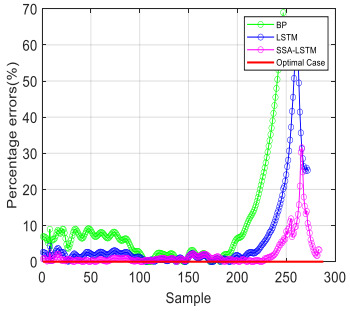

(c) Percentage errors in predicted values

Fig. 7 *v*=200 km/h, response prediction results and error calculation values of bridge mid-span vertical displacement

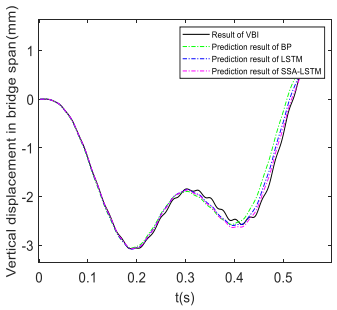

(a) Prediction results

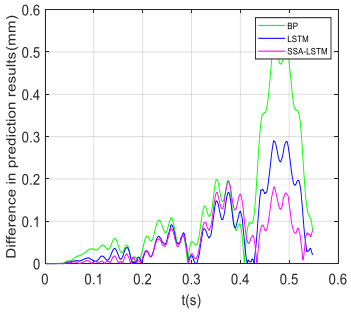

(b) Errors in predicted values

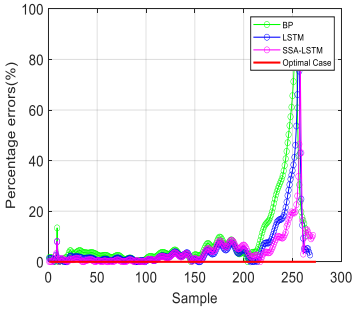

(c) Percentage errors in predicted values

Fig. 8 *v*=210 km/h, response prediction results and error calculation values of bridge mid-span vertical displacement

$$R^2 = 1 - \frac{\sum_{i=1}^{m}\left(y_i - \hat{y}_i\right)^2}{\sum_{i=1}^{m}\left(y_i - \overline{y}_i\right)^2} \tag{27}$$

4. Prediction results of dynamic response of vehicle-bridge interaction system

4.1 Prediction of bridge dynamic response

In engineering practice, the displacement and acceleration responses of bridges are of primary concern. Trained surrogate models can be employed to predict the dynamic responses of both bridges and vehicles. Figs. 7 to 12 illustrate the predicted results of the mid-span vertical displacement and mid-span vertical acceleration responses of the bridge, obtained by different surrogate models under a new set of track irregularity excitations at vehicle speeds of 200 km/h, 210 km/h, and 220 km/h. As shown in these figures, the SSA-LSTM surrogate model

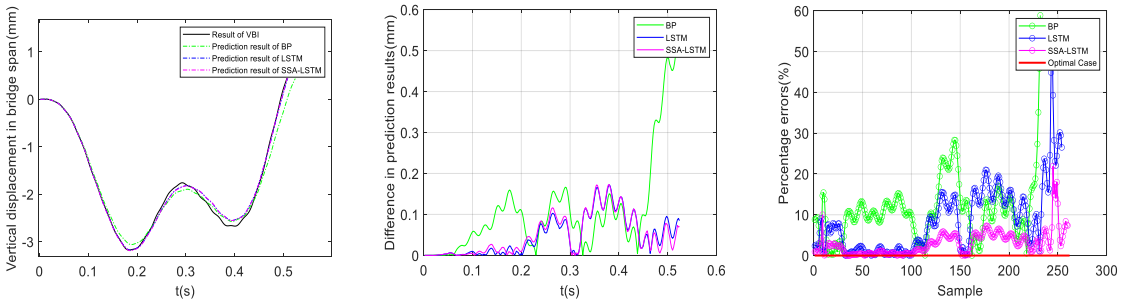

(a) Prediction results (b) Errors in predicted values (c) Percentage errors in predicted values

Fig. 9 v=220 km/h, response prediction results and error calculation values of bridge mid-span vertical displacement

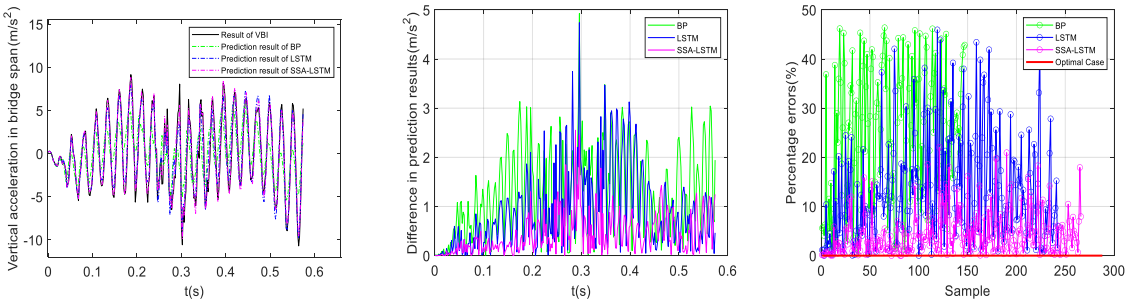

(a) Prediction results (b) Errors in predicted values (c) Percentage errors in predicted values

Fig. 10 v=200 km/h, response prediction results and error calculation values of bridge mid-span vertical acceleration

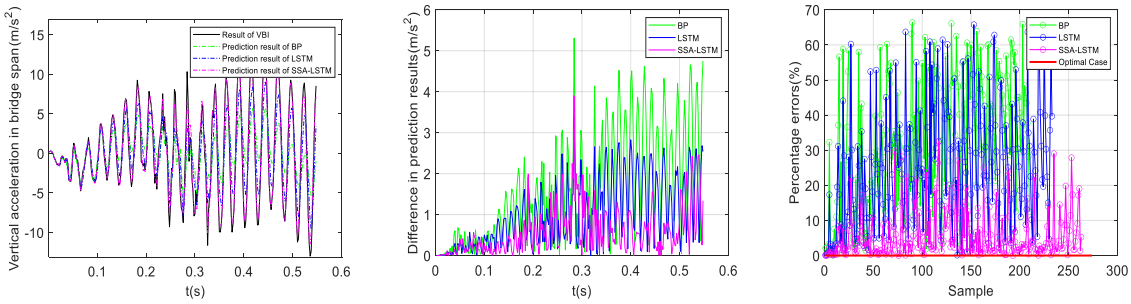

(a) Prediction results (b) Errors in predicted values (c) Percentage errors in predicted values

Fig. 11 v=210 km/h, response prediction results and error calculation values of bridge mid-span vertical acceleration

demonstrates higher prediction accuracy compared to the LSTM and BP surrogate models. This is further supported by Table 1, which presents various evaluation metrics for the prediction of bridge responses using the three surrogate models. The data indicate that the SSA-LSTM model

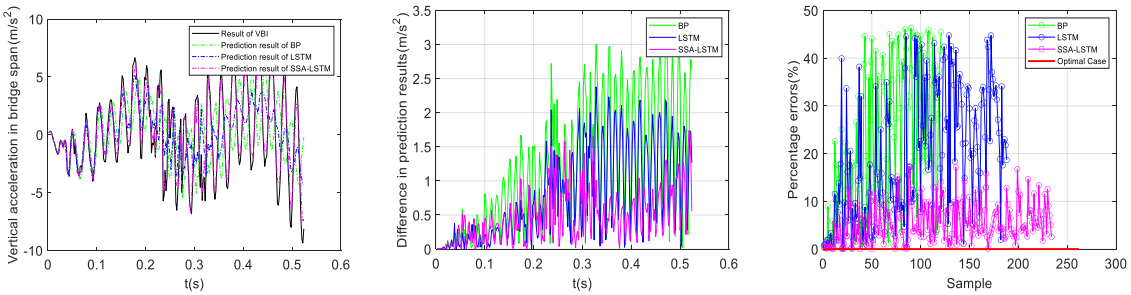

(a) Prediction results (b) Errors in predicted values (c) Percentage errors in predicted values

Fig. 12 v=220 km/h, response prediction results and error calculation values of bridge mid-span vertical acceleration

Table 1 Error index values of three surrogate models for predicting bridge dynamic responses

Vehicle speed	Prediction model	Evaluation indicators for bridge displacement prediction results				Evaluation indicators for bridge acceleration prediction results			
		RMSE	MAE	MAPE	R^2	RMSE	MAE	MAPE	R^2
v=200 km/h	BP	0.160	0.132	25.223%	0.9342	0.068	0.051	30.054%	0.9279
	LSTM	0.121	0.099	8.831%	0.9793.	0.927	0.063	40.571%	0.9194
	SSA-LSTM	0.030	0.021	1.747%	0.9988	0.021	0.015	7.663%	0.9799
v=210 km/h	BP	0.051	0.042	3.413%	0.9667	0.026	0.019	6.824%	0.9689
	LSTM	0.033	0.024	4.036%	0.9686	0.052	0.040	10.639%	0.9558
	SSA-LSTM	0.014	0.011	1.418%	0.9884	0.009	0.007	2.562%	0.9878
v=220 km/h	BP	0.043	0.036	4.062%	0.9681	0.030	0.022	7.770%	0.9394
	LSTM	0.077	0.069	6.987%	0.9640	0.052	0.039	11.399%	0.9212
	SSA-LSTM	0.024	0.020	3.278%	0.9814	0.010	0.008	3.133%	0.9849

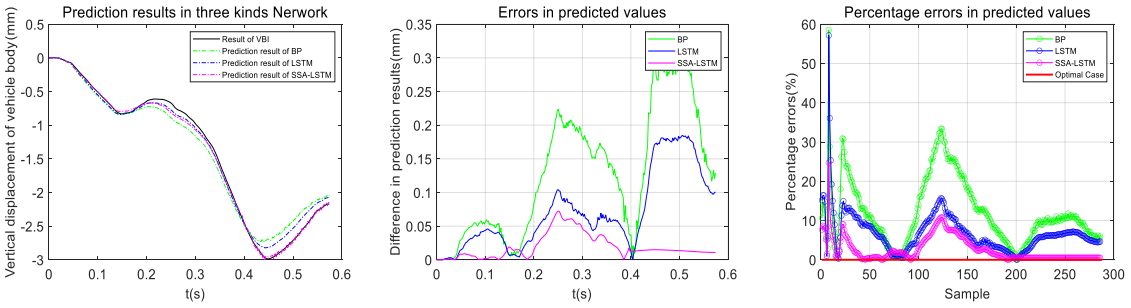

(a) Prediction results (b) Errors in predicted values (c) Percentage errors in predicted values

Fig. 13 v=200 km/h, response prediction results and error calculation values of vehicle body vertical displacement

outperforms the LSTM and BP models in terms of predictive accuracy.

4.2 Vehicle dynamic response prediction

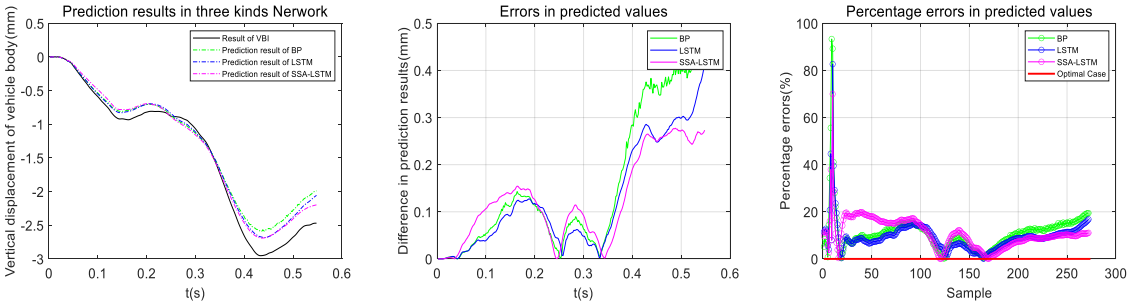

(a) Prediction results (b) Errors in predicted values (c) Percentage errors in predicted values

Fig. 14 *v*=210 km/h, response prediction results and error calculation values of vehicle body vertical displacement

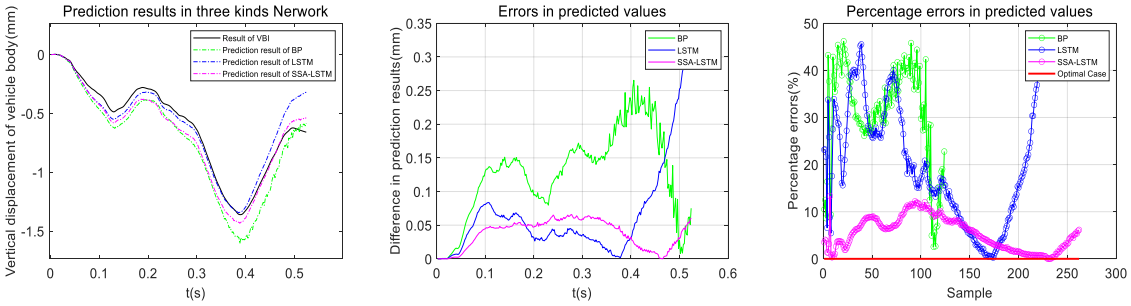

(a) Prediction results (b) Errors in predicted values (c) Percentage errors in predicted values

Fig. 15 *v*=220 km/h, response prediction results and error calculation values of vehicle body vertical displacement

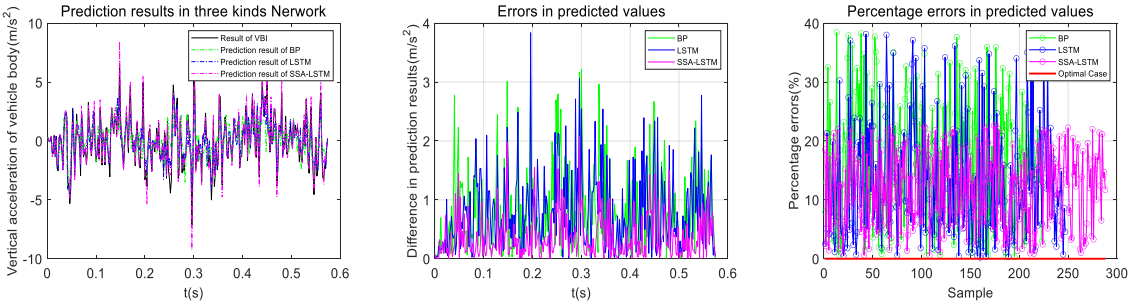

(a) Prediction results (b) Errors in predicted values (c) Percentage errors in predicted values

Fig. 16 *v*=200 km/h, response prediction results and error calculation values of vehicle body vertical acceleration

Figs. 13 to 18 illustrate the predicted results of the vertical displacement and vertical acceleration responses of the vehicle body at speeds of 200 km/h, 210 km/h, and 220 km/h under a new set of track irregularity excitations. As shown in these figures, the SSA-LSTM surrogate

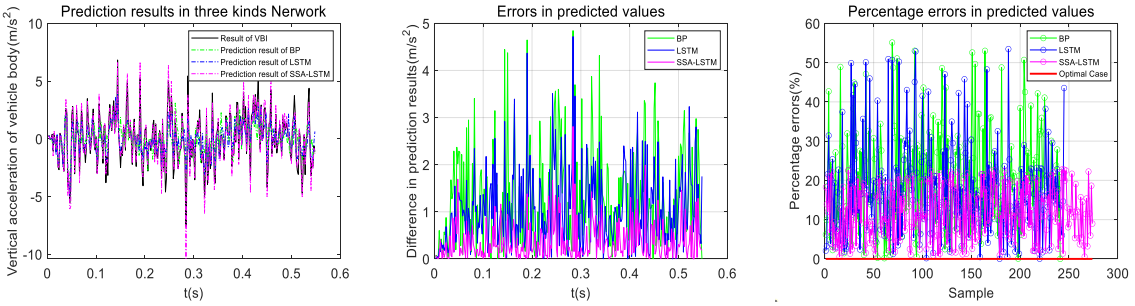

(a) Prediction results (b) Errors in predicted values (c) Percentage errors in predicted values

Fig. 17 *v*=210 km/h, response prediction results and error calculation values of vehicle body vertical acceleration

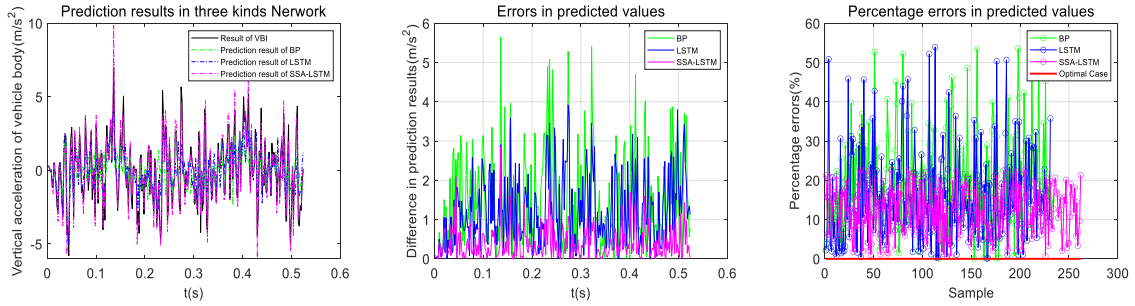

(a) Prediction results (b) Errors in predicted values (c) Percentage errors in predicted values

Fig. 18 *v*=220 km/h, response prediction results and error calculation values of vehicle body vertical acceleration

Table 2 Error index values of three surrogate models for predicting vehicle dynamic responses

Vehicle speed	Prediction model	Evaluation indicators for vehicle displacement prediction results				Evaluation indicators for vehicle acceleration prediction results			
		RMSE	MAE	MAPE	R^2	RMSE	MAE	MAPE	R^2
v=200 km/h	BP	0.050	0.035	3.404%	0.9720	0.025	0.020	8.008%	0.9380
	LSTM	0.030	0.024	4.541%	0.9744	0.015	0.012	4.197%	0.9772
	SSA-LSTM	0.027	0.019	2.001%	0.9893	0.009	0.007	2.088%	0.9912
v=210 km/h	BP	0.100	0.071	5.426%	0.9611	0.212	0.016	7.351%	0.9402
	LSTM	0.117	0.090	9.539%	0.9539	0.027	0.022	4.272%	0.9571
	SSA-LSTM	0.033	0.024	1.730%	0.9800	0.017	0.014	2.882%	0.9888
v=220 km/h	BP	0.049	0.039	4.683%	0.9781	0.0167	0.014	4.090%	0.9384
	LSTM	0.035	0.025	2.441%	0.9885	0.0148	0.011	1.632%	0.9588
	SSA-LSTM	0.028	0.016	1.818%	0.9912	0.0068	0.005	0.474%	0.9897

model achieves higher prediction accuracy compared to the LSTM and BP surrogate models. This is further confirmed by Table 2, which provides a comparison of various evaluation metrics for the prediction of vehicle responses using the three surrogate models. The data clearly demonstrate that

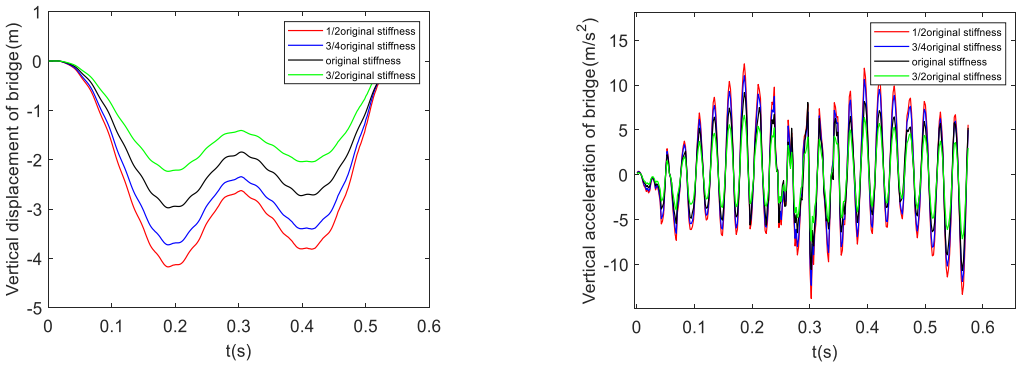

(a) Prediction results of the bridge mid-span vertical displacement

(b) Prediction results of the bridge mid-span vertical acceleration

Fig. 19 Prediction results of bridge dynamic responses under different bridge stiffnesses

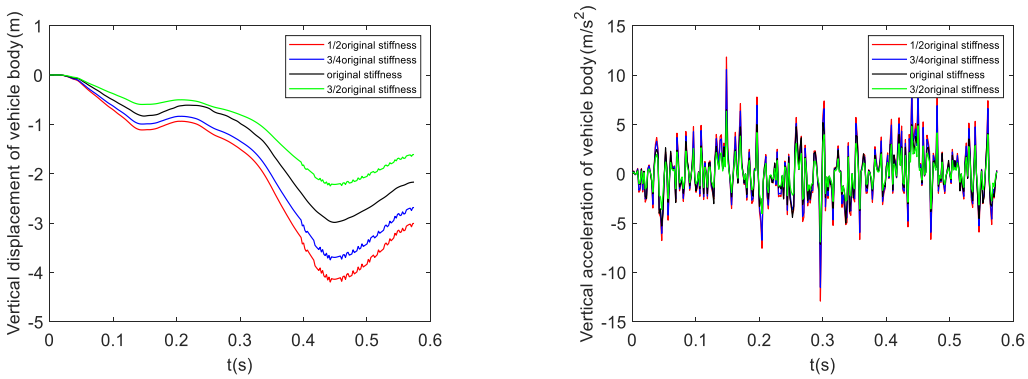

(a) Prediction results of the vertical displacement

(b) Prediction results of the vertical acceleration

Fig. 20 Prediction results of vehicle dynamic responses under different bridge stiffnesses

the SSA-LSTM model outperforms the other two models in terms of predictive performance.

4.3 Prediction and analysis of bridge and vehicle dynamic response under special operating conditions

To further investigate the applicability of surrogate model and comprehensively compare their predictive performance, this section analyzes multiple factors influencing the response of the vehicle-bridge interaction system, including changes in the stiffness and damping of the bridge structure. As the operating speed of China's high-speed EMU trains is mainly 200 km/h, the vehicle speed is set at 200 km/h to analyze the prediction results of the surrogate model for the dynamic response under special working conditions.

4.3.1 Influence of bridge stiffness variation

This section examines the influence of variations in bridge stiffness on the dynamic response prediction outcomes of the vehicle-bridge interaction system. Bridges with stiffness values set at 0.5, 0.75, and 1.5 times the original stiffness were selected for conducting vehicle-bridge

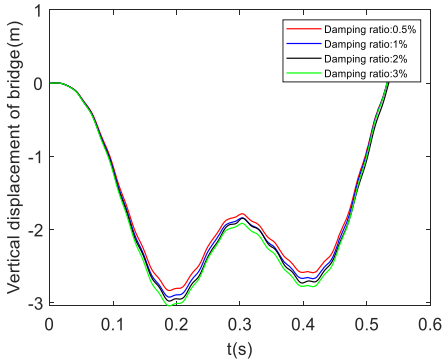

(a) Prediction results of the bridge mid-span vertical displacement

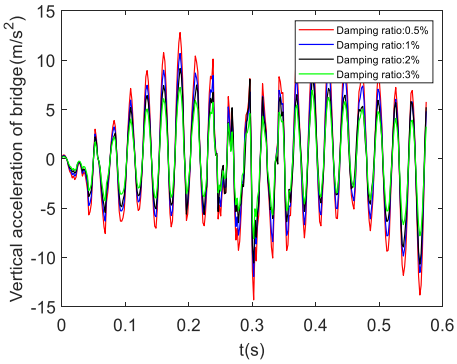

(b) Prediction results of the bridge mid-span vertical acceleration

Fig. 21 Prediction results of bridge dynamic responses under different damping ratios of bridges

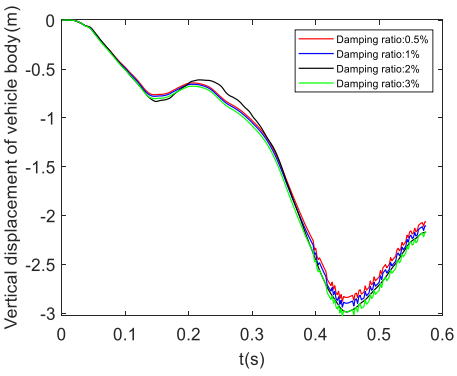

(a) Prediction results of the vertical displacement

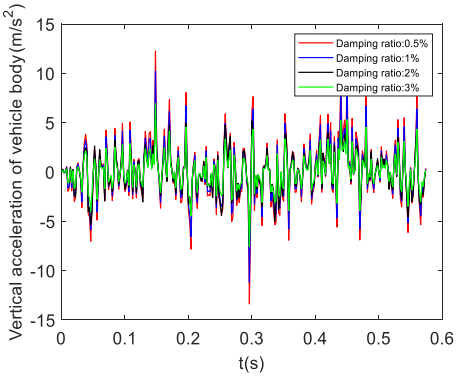

(b) Prediction results of the vertical acceleration

Fig. 22 Prediction results of vehicle dynamic responses under different bridge damping ratios

interaction response analyses, and the resulting data were utilized for training the neural network. The results indicate that bridge stiffness significantly affects the displacement response and acceleration response of both the vehicle and bridge structure, as illustrated in Fig. 19. Specifically, as bridge stiffness decreases, the response magnitudes increase, whereas higher bridge stiffness leads to reduced response values. The surrogate model generates corresponding prediction results, as depicted in Figs. 19-20.

4.3.2 Influence of bridge damping variation

This section examines the influence of variations in bridge damping about the dynamic response prediction outcomes of the vehicle-bridge interaction system. Bridge damping ratios of 0.5%, 1%, 2%, and 3% are considered, and vehicle and bridge coupling model is employed to generate training data to developing the surrogate model. The results demonstrate that the established surrogate model is capable of accurately predicting the displacement and acceleration responses of both the bridge and the vehicle under different damping conditions. Due to the greater sensitivity of the acceleration response to damping variation, while the bridge displacement response exhibits relatively low sensitivity, the predicted displacement response remains largely

unchanged across varying damping levels. In contrast, both the vehicle and bridge acceleration responses exhibit significant variation with damping. Specifically, higher bridge damping results in lower acceleration response values, whereas lower damping leads to increased acceleration responses. The surrogate model generates corresponding prediction results, as illustrated in Figs. 21-22.

5. Conclusions

To enable real-time or near-real-time prediction of the dynamic responses of vehicles and bridges in the vehicle-bridge interaction system, a surrogate model approach is proposed. In this method, the surrogate model replaces the analytical model of the vehicle-bridge interaction system. Based on numerical simulations, a physical model of the system is established, and analytical methods are used to solve for the dynamic responses, which are used to generate training samples and construct the surrogate model. Finally, the surrogate model is employed to predict the displacement and acceleration responses of both the bridge and the vehicle. By comparing the predictive performance of different surrogate models, the following conclusions are drawn:

- A physical model of the vehicle-bridge interaction system is established to achieve real-time or near-real-time prediction of the dynamic responses of bridges and vehicles. This approach effectively integrates measurement data and numerical simulation data, enabling efficient prediction of the system dynamic behavior.
- Given the significant impact of random track irregularity excitation on the dynamic responses of both the bridge and the vehicle during bridge passage, a surrogate model was developed using random track irregularity excitations as input samples and the corresponding dynamic responses of the vehicle or bridge as output samples. This allows for accurate prediction of the system dynamic responses under any given random track irregularity excitation.
- The internal hidden layer parameters of the LSTM neural network were optimized using the Sparrow Search Algorithm (SSA), thereby improving the model prediction accuracy and computational efficiency. The SSA-LSTM surrogate model outperformed both the LSTM and BP surrogate models, with prediction errors generally below 10%. Furthermore, the SSA-LSTM model demonstrated superior performance in predicting the dynamic responses of both the bridge and the vehicle, with the average root mean square error (RMSE) reduced by approximately 38.5%.

Acknowledgements

The research work in this paper was supported by the National Natural Science Foundation of China (Grant No. 51608087), the Open Project of National Engineering Research Center of High-speed Railway Construction Technology in China (No. HSR202010), the Scientific Research Project from the Transportation Department of Liaoning Province in China (No. 2024-09) and the Fundamental Research Funds for the Central Universities in China (No. 3132024170), the Joint Plan Project from Science and Technology Plan of Liaoning Province in China (No. 2025-MSLH-110).

References

Chen, Y. (2022), "Predictions of random response of train on long-span bridge under crosswind based on surrogate model", E.D. Dissertation, Southwest Jiaotong University, Chengdu, China.

Deng, L., Duan, L.L. and He, W. (2018), "Study on vehicle model for vehicle-bridge coupling vibration of highway bridges in China", *Chin. J. Highw. Transp.*, **31**(07), 92-100. https://doi.org/10.3969/j.issn.1001-7372.2018.07.007.

Dong, W. (2019), "Study on vehicle-bridge coupling vibration and impact coefficient based on UM simulation analysis", E.M. Dissertation, Hebei University of Technology, Tianjin, China.

Du, Y.F and Guo, J.H. (2006), "Prediction of structural dynamic response based on RBF neural network", *Journal of Lanzhou University of Technology*, **32**(02), 111-114. https://doi.org/10.3969/j.issn.1673-5196.2006.02.030.

Fang, C., Tang, H.J. and Wang, Z.W. (2020), "Effects of random winds and waves on a long-span cross-sea bridge using Bayesian regularized back propagation neural network", *Adv. Struct. Eng.*, **23**(4), 733-748. https://doi.org/10.1177/1369433219880446.

Gui, S.R., Zhu, C.Y. and Chen, S.S. (2021), "Comparative analysis of dynamic response between continuous rigid frame bridge and continuous bridge with constant cross section and low pier under vehicle", *J. Shenyang Jianzhu Univ. Nat. Sci.*, **37**(04), 685-692. https://doi.org/10.11717/j.issn:2095-1922.2021.04.14.

Han, X. (2022), "Predictions of random response of train on long-span bridge under crosswind based on surrogate model", E.D. Dissertation, Southwest Jiaotong University, Chengdu, China.

He, X., Zhao, Y. and Shi, K. (2025), "BiLSTM-AM: A deep learning model for indirect identification of track irregularity using in-service vehicle acceleration responses", *Int. J. Struct. Stab. Dyn.*, 2541012. https://doi.org/10.1142/S0219455425410123.

He, X.H., Zhao Y.S. and Cai, C.Z. (2024), "Random vibration analysis of vehicle-track- bridge system based on SSA-BP neural network", *J. Railw. Sci. Eng.*, **21**(08), 3225-3236. https://doi.org/10.19713/j.cnki.43-1423/u.T20231756.

Hu, Y. and Guo, W. (2024), "Structural seismic response reconstruction using physics-guided neural networks", *Int. J. Struct. Stab. Dyn.*, **24**(15), 2450171. https://doi.org/10.1142/S0219455424501712.

Kim, T., Kwon, O. and Song, J. (2019), "Response prediction of nonlinear hysteretic systems by deep neural networks", *Neur. Network.*, **111**(C) 1-10. https://doi.org/10.1016/j.neunet.2018.12.005.

Li, H.L., Wang, T.Y. and Wu, G. (2021), "Dynamic response prediction of vehicle-bridge interaction system using feedforward neural network and deep long short-term memory network", *Struct.*, **34**, 2415-2431. https://doi.org/10.1016/j.istruc.2021.09.008.

Li, H.L., Wang, T.Y. and Yan, H. (2023), "Real-time prediction of dynamic irregularity and acceleration of HSR bridges using modified LSGAN and in-service train", *Smart Struct. Syst.*, **31**(5), 501-516. https://doi.org/10.12989/sss.2023.31.5.501.

Li, H.L., Wang, T.Y. and Yang, J.P. (2022), "Deep learning models for time-history prediction of vehicle-induced bridge responses: A comparative study", *Int. J. Struct. Stab. Dyn.*, **23**(01), 2350004. https://doi.org/10.1142/S0219455423500049.

Li, Q., Xu, Y.L. and Chen, Z.W. (2010), "Computer-aided nonlinear vehicle-bridge interaction analysis", *J. Vib. Control*, **16**(12), 1791-1816. https://doi.org/10.13465/j.cnki.jvs.

Li, X.Z. and Wang, M. (2021), "State-of-the-art review of vehicle-bridge interaction vibration in 2020", *J. Civil Environ. Eng.*, **43**(S1), 135-141. https://doi.org/10.11835/j.issn.2096-6717.2021.214.

Li, X.Z., Zhu. Y. and Qiang, S.Z. (2012), "Stochastic response analysis of train-bridge interaction system under high-speed train loads excitation", *J. Vib. Shock*, **31**(04), 168-172. https://doi.org/10.3969/j.issn.1000-3835.2012.04.032.

Li, Y.H. (2023), "Dynamic response analysis of vehicle-bridge interaction system based on Ansys-UM co-simulation", E.M. Dissertation, Dalian Maritime University, Dalian, China.

Li, Y.L., Xiang, H.Y. and Qiang, S.Z. (2018), "Review on interaction vibration of wind-vehicle bridge systems", *Chin. J. Highw. Transp.*, **31**(07), 24-37. https://doi.org/10.3969/j.issn.1001-7372.2018.07.002.

Liao, Y.C. and Zhang, R.Y. (2024), "A stacked residual lstm network for nonlinear seismic response prediction of bridges", *Eng. Mech.*, **41**(04), 47-58. https://doi.org/10.6052/j.issn.1000-4750.2022.04.0360.

Liu, Z.J., Zhang, C.Y. and Qi, D.C. (2018), "Probability density evolution method for the ride comfort evaluation of high-speed trains", *J. Vib. Shock*, **37**(14), 149-155. https://doi.org/10.13465/j.cnki.jvs.2018.14.020.

Malekjafarian, A., McGetrick, P.J. and OBrien, E.J. (2015), "A review of indirect bridge monitoring using passing vehicles", *Shock Vib.*, **2015**(1),1-16. https://doi.org/10.1155/2015/286139.

Mao, J.F., Li, Z. and Wu, J. (2024), "A method for predicting random vibration response of heavy-haul train-track-bridge system based on PSO-LSTM", *J. Railw. Sci. Eng.*, **21**(09), 3661-3671. https://doi.org/10.19713/j.cnki.43-1423/u.T20232004.

Ni, Y.H., Mao, J.X. and Fu, Y.H. (2023), "Damage detection and localization of bridge deck pavement based on deep learning", *Sensor.*, **23**(11), 5138. https://doi.org/10.3390/s23115138.

Ning, F. and Deng, N.C. (2024), "Analysis of vehicle-bridge-support coupling dynamic response of simply supported beam based on Ansys", *Sci. Technol. Indus.*, **24**(06), 287-294. https://doi.org/10.3969/j.issn.1671-1807.2024.06.041.

Rocha, J.M., Henriques, A.A. and Calcada, R. (2015), "Methodology for the probabilistic safety assessment of high-speed railway bridges", *Eng. Struct.*, **101**(15), 138-149. https://doi.org/10.1016/j.engstruct.2015.07.020.

Shi, K., Yang, Y.B. and Mo, X.Q. (2025), "Study of vehicle scanning method for bridge mode shape identification by using the PSO-HT algorithm", *J. Bas. Sci. Eng.*, **33**(01), 1-11. https://doi.org/10.16058/j.issn.1005-0930.2025.01.001.

Simpson, T.W., Poplinski, J.D., Koch, P.N. and Allen, J.K. (2001), "Metamodels for computer-based engineering design: Survey and recommendations", *Eng. Comput.*, **17**(2), 129-150. https://doi.org/10.1007/PL00007198.

Tang, Z., Dong, S.D. and Luo, R. (2021), "Application advances of artificial intelligence algorithms in dynamics simulation of railway vehicle", *J. Traff. Transp. Eng.*, **21**(01), 250-266. https://doi.org/10.19818/j.cnki.1671-1637.2021.01.012.

Wang, H. and Wu, T. (2020), "Knowledge-enhanced deep learning for wind-induced nonlinear structural dynamic analysis", *J. Struct. Eng.*, **146**(11), 14. https://doi.org/10.1061/(ASCE)ST.1943-541X.000280.

Wang, W. (2019), "Random dynamic analysis and running safety reliability evaluation of vehicle-track (bridge) interaction systems", E.D. Dissertation, Dalian University of Technology, Dalian, China.

Wang, X.W. and Tan, J.D. (2003), "Application and developing trends of neural network", *Comput. Eng. Appl.*, **113**(03), 98-100. https://doi.org/10.3321/j.issn:1002-8331.2003.03.033.

Wang, Z.L., Yang, J.P. and Shi, K. (2022), "Recent advances in researches on vehicle scanning method for bridges", *Int. J. Struct. Stab. Dyn.*, **22**(15), 2230005. https://doi.org/10.1142/S0219455422300051.

Xia, H., Zhang, H.J. and Cao, Y.M. (2003), "Dynamic analysis of train-bridge system under random excitations", *Eng. Mech.*, **20**(03), 142-149. https://doi.org/10.3969/j.issn.1000-4750.2003.03.025.

Xiao, X.B. and Shen, H.M. (2005), "Dynamic simulation of bridge subjected to moving load", *J. Vib. Shock*, **142**(01), 123-125. https://doi.org/10.3969/j.issn.1000-3835.2005.01.032.

Xiao, X.B. and Shen, H.M. (2005), "Dynamic simulation of bridge subjected to moving load", *J. Vib. Shock*, **142**(01), 123-125. https://doi.org/10.3969/j.issn.1000-3835.2005.01.032.

Xiao, Y.G. and Zhu, S.H. (2007), "Nonlinear dynamic analysis of vehicle bridge coupled interaction system", *J. Vib. Shock*, **173**(08), 104-108. https://doi.org/10.3969/j.issn.1000-3835.2007.08.026.

Xu, Z.K. and Chen, J. (2021), "Neural network algorithm for nonlinear structural seismic response", *Eng. Mech.*, **38**(09), 133-145. https://doi.org/10.6052/j.issn.1000-4750.2020.09.0645.

Yang, Y.B. and Yang, J.P. (2017), "State-of-the-art review on modal identification and damage detection of bridges by moving test vehicles", *Int. J. Struct. Stab. Dyn.*, **18**(2), 1850025. https://doi.org/10.1142/S0219455418500256.

Yang, Y.B., Lin, C.W. and Yau, J.D. (2004), "Extracting bridge frequencies from the dynamic response of a passing vehicle", *J. Sound Vib.*, **272**(3-5), 471-493. https://doi.org/10.1016/s0022-460x(03)00378-x.

Yu, Z.W. and Mao, J.F. (2015), "The stochastic analysis of the track-bridge vertical interaction vibration

with random train parameters", *J. Chin. Railw. Soc.*, **37**(01), 97-104. https://doi.org/10.3969/j.issn.1001-8360.2015.01.015.

Zhang, J.F., Wu, C. and Fang, Y. (2024), "Dynamic response analysis of rigid frame continuous composite beam bridge based on vehicle-bridge coupling", *J. Chengdu Univ.*, **43**(04), 430-436. https://doi.org/10.3969/j.issn.1004-5422.2024.04.015.

Zhou, Y.J., Xue, Y.X. and Gao, X.J. (2023), "Research on dynamic amplification factor of highway simply supported girder bridge based on modal superposition method", *J. Traff. Transp. Eng.*, **23**(06), 146-155. https://doi.org/10.19818/j.cnki.1671-1637.2023.06.008.

Zhu, D.Y., Zhang, Y.H. and Kennedy, D. (2014), "Stochastic vibration of the vehicle-bridge system subject to non-uniform ground motions", *Vehic. Syst. Dyn.*, **52**(3), 410-428. https://doi.org/10.1080/00423114.2014.886707.